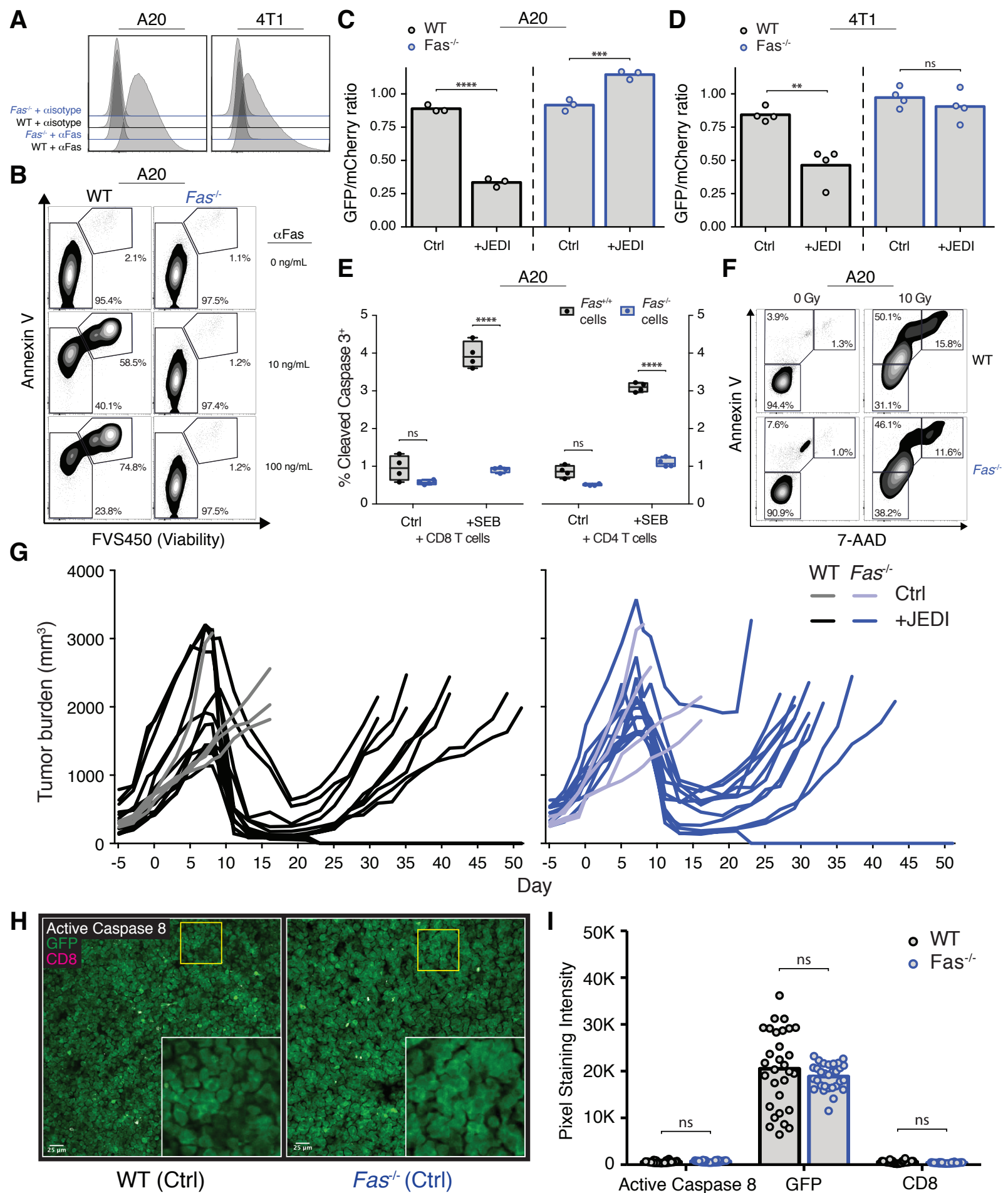
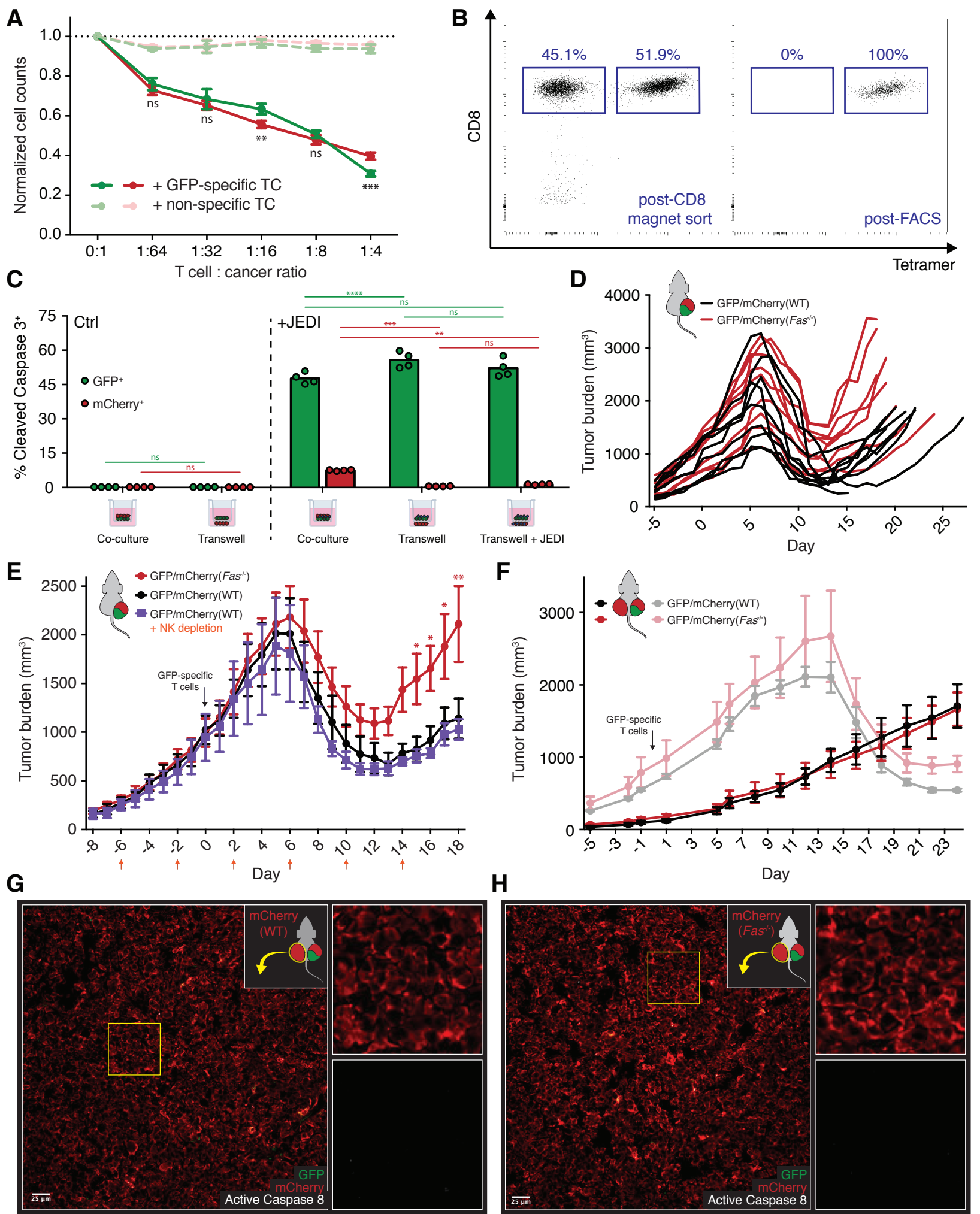


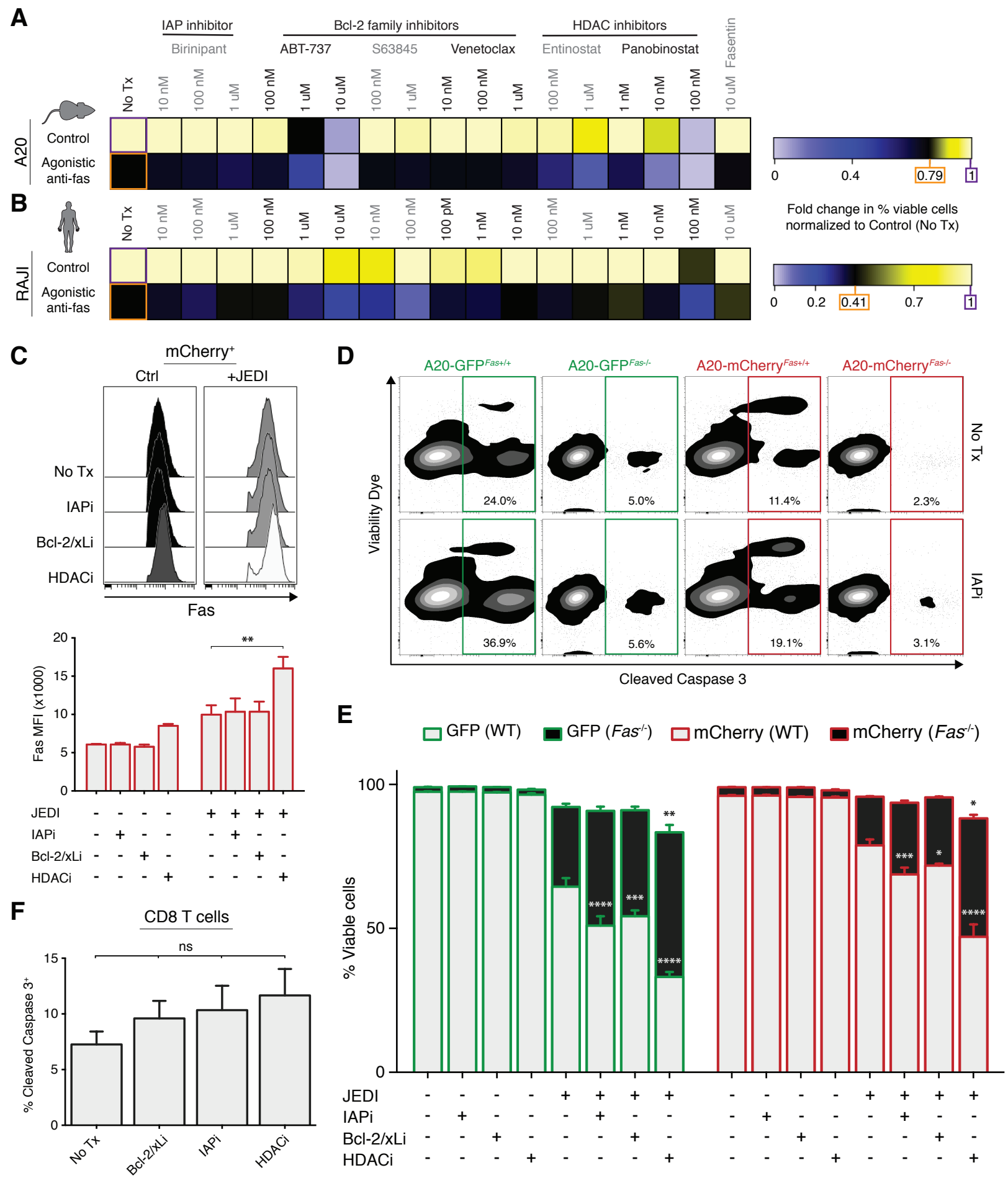
**Supplementary Figure S1. CRISPR/Cas9 knockout of *B2m*, *Tap1*, and *Fas* protects A20 lymphoma from CD8 T cell killing.** **A**, Representative changes in ratio of surviving GFP<sup>+</sup> and mCherry<sup>+</sup> cells after 1 iteration of selection with JEDI T cells. **B**, Cumulative frequency distribution of integrated small guide targeting RNA sequences from genomic DNA of indicated samples from a representative library; ‘All other samples’ include GFP<sup>+</sup> and mCherry<sup>+</sup> cells from Baseline, Ctrl (Iteration 1), JEDI (Iteration 1), and Ctrl (Iteration 2); data shown are medians (n=5). **C**, Standardized residuals of a linear regression function (F-statistic = 4856) of percent reads for each sgRNA target in GFP<sup>+</sup> population against paired reads in mCherry<sup>+</sup> population; dashed lines represent Z-score thresholds of  $\pm 2.58$ ; select targets (p<0.01) out of total 5,186 data points highlighted in red. **D-E**, Percent of all sequenced reads mapping to each of 4 small guide RNA sequences (alternating purple and orange shading) targeting *B2m* (**D**) and *Tap1* (**E**) across all samples; boxplots presented as minimum to maximum; two-way ANOVA with Sidak correction for multiple comparisons, \*\*p<0.01, \*\*\*\*p<0.0001 (n=5). **F**, Representative surface expression distribution of MHC Class I and PD-L1 of GFP<sup>+</sup> (right panel) and mCherry<sup>+</sup> (left panel) cells after 3 iterations of selection with JEDI T cells in a library containing 4 small guide RNAs targeting *B2m* and *Cd274*. **G-H**, Percent of all GFP<sup>+</sup> and mCherry<sup>+</sup> cells from **F** in negative gate of MHC Class I (**G**) or PD-L1 (**H**); unpaired t-test (n=5). **I**, Percent of all sequenced reads mapping to each of 4 small guide RNA sequences (alternating purple and orange shading) targeting *Fas* across all samples; boxplots presented as minimum to maximum; two-way ANOVA with Sidak correction for multiple comparisons, \*\*\*\*p<0.0001 (n=5).



**Supplementary Figure S2. *Fas*<sup>-/-</sup> cancer is resistant to killing by multiple model T cell systems despite comparable susceptibility to radiation-induced apoptosis.** **A**, Relative surface staining intensity for WT (black) and *Fas*<sup>-/-</sup> (blue) A20 (left panel) and 4T1 (right panel) cell lines using APC-conjugated anti-Fas (clone SA367H8) or anti-IgG1k isotype control. **B**, Representative apoptosis induced in WT (left panel) and *Fas*<sup>-/-</sup> (right panel) A20 cells after 48-hour incubation with agonistic anti-Fas (clone Jo2) at the indicated concentrations. **C-D**, Ratio of GFP<sup>+</sup>:mCherry<sup>+</sup> A20 (**C**) or 4T1 (**D**) cells from Fig. 1D-E; error bars presented as mean ± SEM; two-way ANOVA with Sidak correction for multiple comparisons, \*\*p<0.01, \*\*\*p<0.001, \*\*\*\*p<0.0001 (n=3-4). **E**, Percent of dying WT (black) or *Fas*<sup>-/-</sup> (blue) A20 lymphoma cells after co-culture with freshly isolated CD8 (left panel) or CD4 (right panel) T cells from balb/c mice in the presence of 50 ng/mL bacterial superantigen SEB; boxplots presented as minimum to maximum; two-way ANOVA with Sidak correction for multiple comparisons, \*\*\*\*p<0.0001 (n=4). **F**, Representative early (Annexin V<sup>+</sup>, 7-AAD<sup>-</sup>) and late (Annexin V<sup>+</sup>, 7-AAD<sup>+</sup>) apoptosis staining of WT or *Fas*<sup>-/-</sup> A20 lymphoma cells 48 hours after irradiation with indicated doses. **G**, Individual tumor curves from Fig. 1G; 3 out of 12 WT tumors cured (black) and 1 out of 12 *Fas*<sup>-/-</sup> tumors cured (blue); pooled from 2 independent experiments. **H**, Representative confocal IF of tumors cryopreserved from 'Ctrl' groups from Fig. 1G on day 8; area outlined in yellow magnified in inset. **I**, Quantification of fluorescent intensities from 30 fields of view as shown in **H**; pixel staining intensity units on a scale from 0 to 65,536 (16-bit); two-way ANOVA with Sidak correction for multiple comparisons (n=3-4 mice/group, pooled from 3 independent experiments).

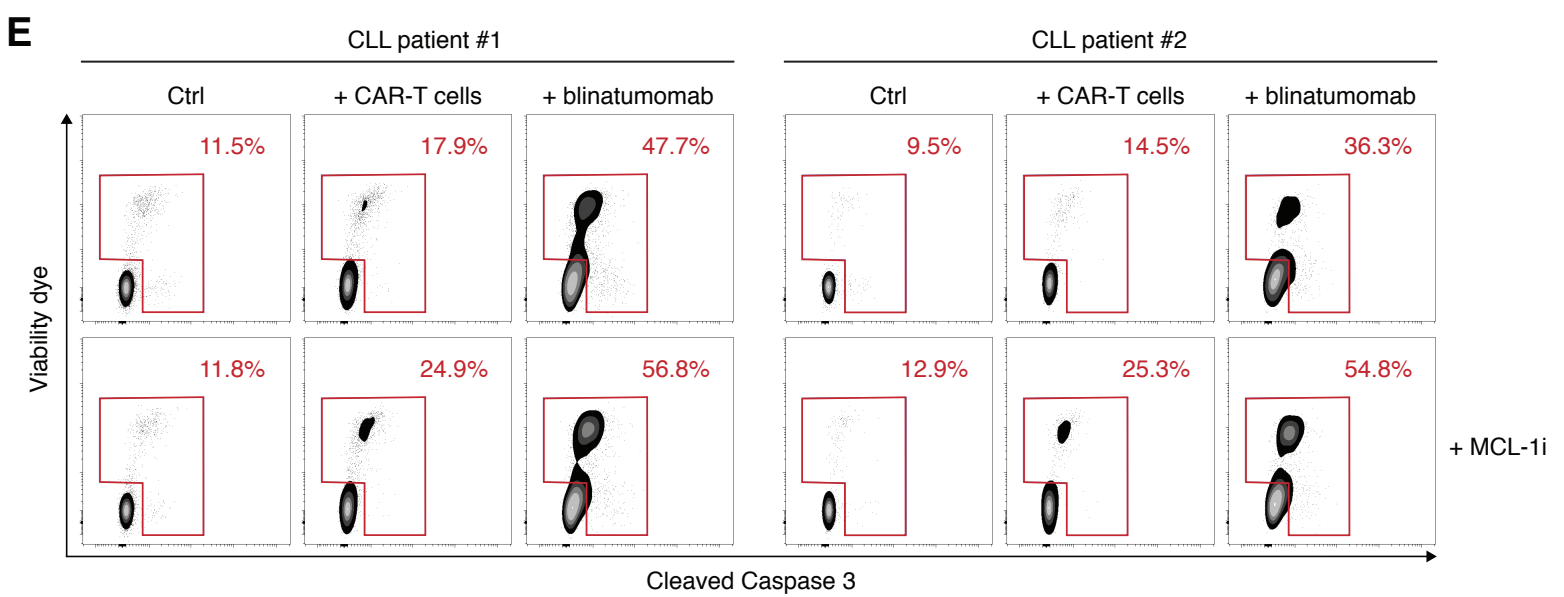
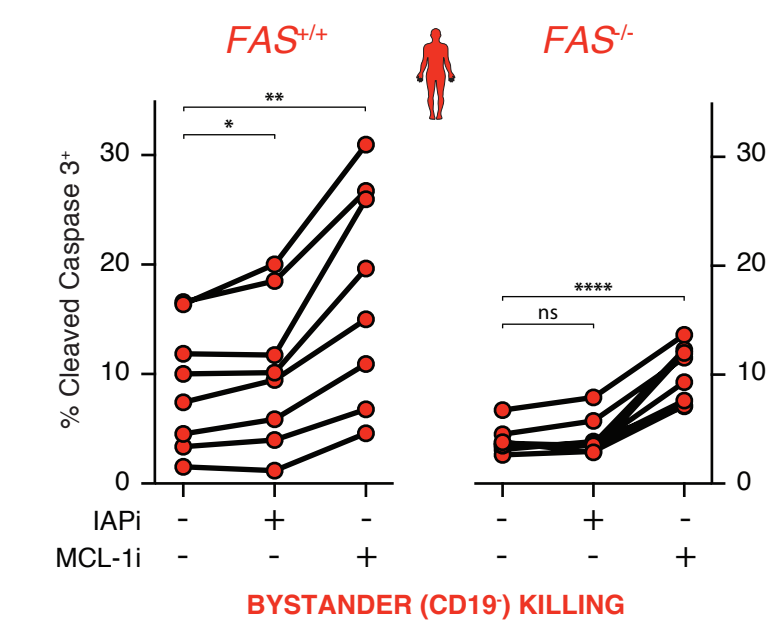
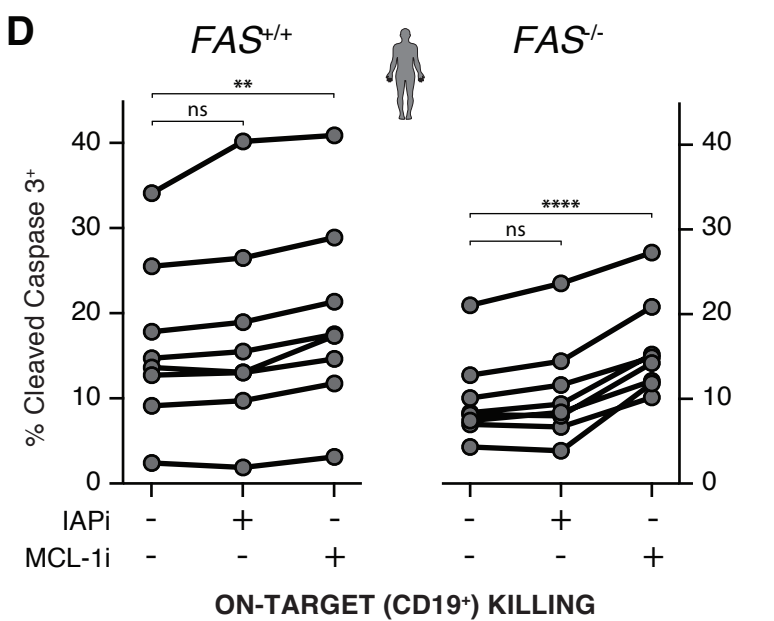
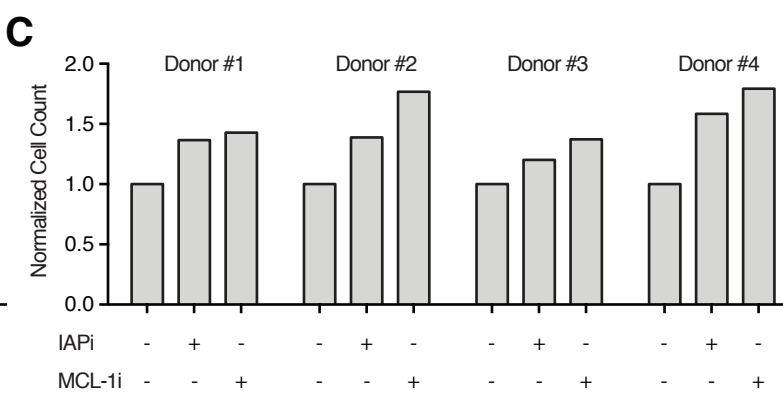
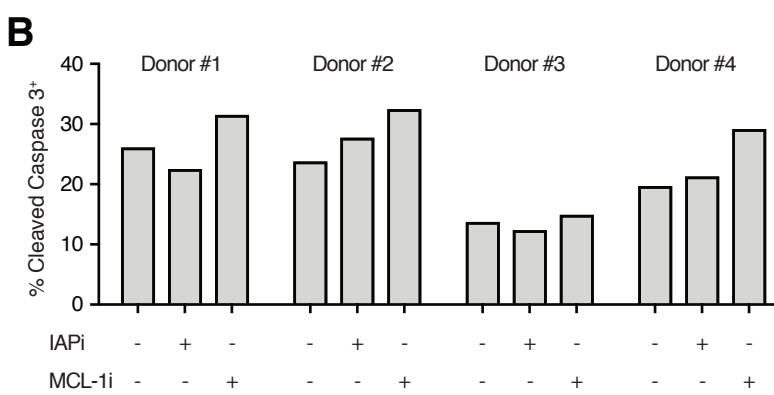
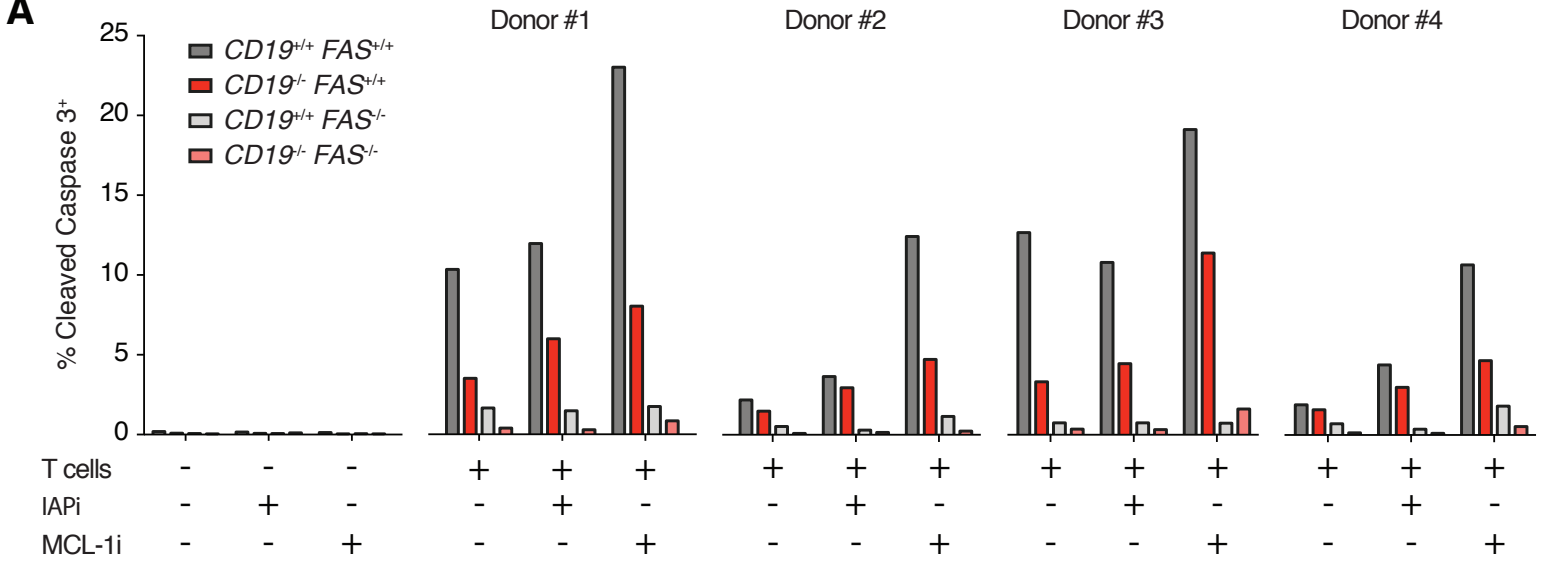


**Supplementary Figure S3. *In vivo* bystander killing by T cells is dependent on proximity to Ag<sup>+</sup> cells.** **A**, Cell counts of *Fas*<sup>-/-</sup> GFP<sup>+</sup> (green) and WT mCherry<sup>+</sup> (red) cells co-cultured with FACS purified tetramer<sup>+</sup> (dark, GFP-specific) or tetramer<sup>-</sup> (light, non-specific) activated CD8 T cells at indicated ratios; counts relative to beads and normalized to 0:1 condition; error bars presented as mean ± SEM; two-way ANOVA with Sidak correction for multiple comparisons, \*\*p<0.01, \*\*\*p<0.001 (n=4). **B**, Representative population of T cells used in killing assays by negative enrichment magnet sorting (left panel; 97% CD8 T cells with 52% of cells specific for GFP antigen) or after tetramer-based FACS (right panel; 100% CD8 T cells with 100% specificity for GFP antigen). **C**, Mean of cells positive for cleaved caspase 3 within GFP<sup>+</sup> (green) and mCherry<sup>+</sup> (red) populations from Fig. 2B; two-way ANOVA with Sidak correction for multiple comparisons, \*\*p<0.01, \*\*\*p<0.001, \*\*\*\*p<0.0001 (n=4). **D**, Individual tumor curves from Fig. 2D; pooled from 2 independent experiments. **E**, Growth of mixed tumors with 50% WT GFP<sup>+</sup> cells and 50% WT mCherry<sup>+</sup> cells in untreated (black) or natural killer cell-depleted (purple) *Rag1*<sup>-/-</sup> mice adoptively transferred with tetramer-sorted GFP-specific CD8 T cells (black arrow); a cohort of mixed tumors with *Fas*<sup>-/-</sup> mCherry<sup>+</sup> cells is shown for comparison (red); anti-asialo-GM1 treatment for NK-depletion indicated with orange arrows; error bars presented as mean ± SEM; two-way ANOVA with Sidak correction for multiple comparisons, \*p<0.05, \*\*p<0.01 (n=4-5 mice/group). **F**, Tumor growth in *Rag1*<sup>-/-</sup> mice bearing mixed primary GFP<sup>+</sup>/mCherry<sup>+</sup> tumors (light shaded curves) and distant secondary mCherry<sup>+</sup> tumors (dark shaded curves) with either WT (black) or *Fas*<sup>-/-</sup> (red) mCherry<sup>+</sup> cells; distant tumors inoculated 10 days after primary tumors; error bars presented as mean ± SEM; two-way ANOVA with Sidak correction for multiple comparisons (n=6 mice/group). **G-H**, Representative confocal IF images of distant tumors from **F** with insets showing magnified single channel images of area outlined in yellow; arrows point to areas of active caspase 8 staining (bottom insets) and corresponding areas in the mCherry channel (top insets).



**Supplementary Figure S4. Targeting inhibitors of apoptosis proteins (IAP), Bcl-2 family members, and histone deacetylases (HDACs) potentiates fas-mediated T cell cytotoxic activity.** **A-B**, Percent of viable murine A20 (**A**) and human Raji (**B**) cells after 48 hour incubation with agonistic antibody to fas and concurrent treatment with the indicated small molecule inhibitors; viability determined by negative staining for exclusion dye FVS780; coloring bar standardized to conditions outlined in purple and orange as indicated. **C**, Surface fas expression on WT mCherry<sup>+</sup> cells (top panel) from co-culture conditions in Fig. 3D and quantification of mean fluorescent intensities (bottom panel); error bars presented as mean  $\pm$  SEM; two-way ANOVA with Sidak correction for multiple comparisons, \*\* $p < 0.01$  (n=3). **D**, Gating for data in Fig. 3D and representative percent of dying cells after 2 day co-culture of 4 cancer cell populations (columns) with JEDI T cells, untreated (top row) or with 1  $\mu$ M birinapant (bottom row). **E**, Percent of WT (gray) or *Fas*<sup>-/-</sup> (black) GFP<sup>+</sup> (green, left panel) and mCherry<sup>+</sup> (red, right panel) cells negative for viability exclusion dye FVS780 after 2 day co-culture with JEDI T cells, 1  $\mu$ M birinapant (IAPi), 100 nM ABT-737 (Bcl-2/xLi), and/or 1 nM panobinostat (HDACi); error bars presented as mean  $\pm$  SEM; indicated statistics relative to 5th column of each panel; two-way ANOVA with Sidak correction for multiple comparisons, \* $p < 0.05$ , \*\* $p < 0.01$ , \*\*\* $p < 0.001$ , \*\*\*\* $p < 0.0001$  (n=3). **F**, Percent of dying CD8 T cells from co-culture conditions in Fig. 3D; error bars presented as mean  $\pm$  SEM; repeated measure one-way ANOVA with Sidak correction for multiple comparisons (n=3).





**Supplementary Figure S5. The efficacy of on-target and bystander killing in blinatumomab and CAR-T cell therapy can be potentiated with small molecule modulators of the fas pathway.** **A**, Percent of dying target Raji cells after co-culture with purified human CD8 T cells from healthy donors in the presence of 100 pM blinatumomab and treated with 100 nM birinapant (IAPi) or 10 nM S63845 (MCL-1i); healthy donor data individualized from aggregate data depicted in Fig. 3E and 3F. **B-C**, Percent of dying (**B**) and normalized cell counts (**C**) of CD8 T cells from co-culture conditions described in **A**. **D**, Percent of dying *CD19<sup>+/+</sup>* on-target (gray; left panel) and *CD19<sup>-/-</sup>* bystander (red; right panel) Raji cells when co-cultured with human CD19-targeting CAR-T cell product for 6 hours concurrently with 100 nM birinapant (IAPi) or 10 nM S63845 (MCL-1i); matched data points from each healthy donor CAR-T cell product connected by lines; repeated measure one-way ANOVA with Holm-Sidak correction for multiple comparisons, \* $p < 0.05$ , \*\* $p < 0.01$ , \*\*\*\* $p < 0.0001$  (n=8). **E**, Percent of apoptotic chronic lymphocytic leukemia (CLL) cells from 2 independent patients (left and right panels) after 2 day co-culture with human CAR-T cell product alone or an equal number of peripheral CD8 T cells from a healthy donor and 1 nM blinatumomab; primary target cells labeled with cytoplasmic CellTrace dye for gating; MCL-1i = 10 nM S63845.